

Original Article

Design, Simulation & Load Prediction of Resilient Nano-Grid for Coastal Household

Vighnesh Binoy¹, Shankar Nalinakshan^{2*}, Akash Kinattinkara³, Anudev J⁴

^{1, 2, 3, 4}Department of Electrical and Electronics Engineering, Amrita Vishwa Vidyapeetham, Amritapuri, India.

*Corresponding Author : shankarnalinakshan@am.amrita.edu.

Received: 01 September 2025

Revised: 03 October 2025

Accepted: 02 November 2025

Published: 28 November 2025

Abstract - As the hazards associated with both natural and artificial threats continue to increase, nano-grids have become increasingly important as a crucial component for guaranteeing the continuous supply of energy. Nano-grids are proving to be an effective method of integrating decentralized renewable energy sources when the utility grid is in operation. This research deals with the design and simulation of a Nano-grid along with the electric load prediction for 24 hours in advance using an ARIMA-XGBoost ensemble model. The model performs exceptionally well when compared to the individual ARIMA and XGBoost models, according to evaluations using the Mean Absolute Error (MAE), Root Mean Square Error (RMSE), and Mean Absolute Percentage Error (MAPE) metrics. Values of MAE, RMSE, and MAPE are 260.41, 277.72, and 13.67% respectively. The predictions are employed in the proposed model to regulate the modes of operation of the Nano-grid. Existing research works have not focused on controlling power flow in a Nano grid using an AI-based technique. In the proposed work, a novel ARIMA-XGBoost ensemble algorithm is used for controlling power flow in a Nano-grid. Therefore, this approach contributes to both automation and increased grid resilience.

Keywords - ARIMA, Hybrid model, Nano-grid, Resiliency, XGBoost.

1. Introduction

The growing usage of inconsistent power sources and the growth of the electric power grid have been linked to several problems, including the requirement for expensive transmission lines and the problem of cumulative blackouts, which can negatively impact vital infrastructures. Microgrids, which provide a steady supply of power to loads, are generally acknowledged as a practical way to increase grid resilience and dependability [1]. A crucial component of microgrid operations is predictive maintenance, which enables it to anticipate possible equipment failures, minimize downtime, and boost system performance. The precision of failure predictions, real-time problem detection and diagnosis, and the overall wellness and remaining useful life of network components can all be greatly enhanced by machine learning-based approaches [2]. The frequency of large-scale disturbances is increasing at a startling rate on a global scale. Because of this, enhancing modern power utilities' ability to withstand low-probability and high-impact calamities is the top goal. In this regard, the core elements of the smart grid, or Nano-grids, offer fascinating methods for improving the robustness of the distribution system through the integration and accommodation of diverse distributed energy sources. In remote, sparsely populated places, Nano-grids are dependable. Nano-grid-based solutions are the subject of research to create a more reliable electrical supply. To supply loads locally

during extreme events, these methods primarily depend on micro-grids functioning independently. Numerous tactics have been created to accomplish this goal. The majority of strategies use machine learning models to determine limitations, and those constraints are then used to achieve the goal of microgrid resilience. The proposed model uses an ARIMA-XGBoost ensemble model to predict the electric load 24 hours ahead of time. As a result, our strategy promotes automation and improved grid resilience. Existing research works have not focused on controlling power flow in a Nano-grid using an AI-based technique. In the proposed work, a novel ARIMA-XGBoost ensemble algorithm is used for controlling power flow in a Nano-grid.

2. Literature Survey

Micro Grids (MG) are technologies that give users efficient and sustainable energy. A significant portion of distributed energy resources that are based on renewable energy and have power electronics interfaces are used by the MG [3]. Since wind and solar energy are sporadic, hybrid systems are usually utilized to enhance resource efficiency and reduce net costs, as well as to complement a single renewable energy-based producing option [4]. MG needs a framework for making decisions in order to function effectively. We must first do a morphological examination of the suggested design. Following that, datasets from various real-world MG



structures may be recovered. Patterns in this data can be found using AI methods like neural networks [5]. An integer-based linear program may be used to construct MG for both cost reduction and the best possible load distribution. The formulation's decision factors include distributed power generation, photovoltaic system sizing, power storage system sizing, and distributed generating system hourly dispatch. Energy collectors and device performance are reassessed in both grid-connected and islanded modes [6].

Including probabilistic data on fragility, hazards, and severe events in a power-distribution model is crucial for control. The power system failure probability may be calculated with the tool. The hourly representative results are converted into input parameters for the suggested optimization model by using a k-means clustering technique on a climatic dataset of the population being studied [7-12]. Six operating scenarios are examined in order to determine the best hybrid MG design: (1) A continuous power supply that runs around the clock; (2) The percentage of load shedding; (3) Curtailment of diesel power generators (gensets); (4) The worst weather conditions; (5) The use of energy from renewable sources, such as Battery Energy Storage Systems (BESSs); and (6) The use of gensets. The suggested optimization model is solved using an Approximate Mathematical Programming Language (AMPL) tool [13]. As the number of sources of Renewable Energy System (RES) increases, advanced technologies for connecting RES are being researched. For this, MGs present a possible answer.

MGs use a single programmable system made up of a cluster of loads and micro sources to supply power and heat to a local area. The radial distribution system, combined with renewable energy technology, converts the same power source into several bidirectional power sources. With this concept, radial distribution systems and the power outages they cause are decreased, and system dependability is raised. The greatest potential is determined by comparing several additional aspects, including demand side management, energy efficiency, carbon dioxide emissions, power system stability, computer applications, and economic assessment [14]. Intelligent management that communicates with the equipment through wired or wireless protocols is another feature of a typical MG system [15]. The lack of inertia and parameter uncertainty make designing control mechanisms for islanded MGs extremely difficult [16]. A thorough synthesis of their interrelationships and resiliency techniques is lacking in existing research, which frequently isolates elements or control mechanisms. Key MG subtypes, including islanded, hybrid approaches, multi-energy, and self-regulating systems, should be identified by the research efforts. Additionally, the impact of vital elements such as energy storage facilities and distributed energy resources in boosting resilience should be assessed [17]. For decentralized demand administration and local energy trading activities in an MG with renewable energy resources, direct communication functionalities are a

crucial component [18-22]. PV panels generate electrical energy by converting sunlight to Direct Current (DC). The system requires a Buck-Boost Converter to regulate the power outputs that flow between the PV Unit and Battery. To store additional energy, batteries are added. Inverters are used to convert DC energy that comes from the batteries and solar panels into AC power [23]. PV modules struggle to sustain efficiency in a variety of environmental situations, despite their potential [24].

The study proposes and examines the hybrid storage of energy and demand response solutions as more dependable mitigation options to handle the PV system's intermittency. These approaches present viable ways to incorporate sporadic renewable energy sources into the system [25]. Weather variations provide a serious obstacle to Photovoltaic (PV) systems' ability to efficiently capture the maximum solar energy. PV systems that seek to maximize power production during Maximum Power Point Tracking (MPPT), particularly in Partial Shading Conditions (PSCs), have an exceptionally difficult task. The PSCs produce one global peak and several local peaks in the PV arrays' P-V curve. To determine the global peak, guarantee the maximum power output point, and prevent entrapment in the local peaks, complex MPPT optimization algorithms must be used. Because of its dependability and simplicity, the Perturb & Observe (P&O) MPPT is frequently used in Photovoltaic (PV) systems [24]. Evaluating the power and then contrasting it to the prior value is how one determines the power change following a disrupted operation.

The process continues in the direction of the perturbation, which is the elevated voltage, when ΔP is larger than 0. The operation must respect the perturbation direction, which is the reduced voltage, to achieve MPP. The direction of the prior adjustment and the trajectory of the previous perturbation are the two main factors on which the P&O approach depends on. To achieve optimal control of the MPPT using the P&O approach, it is helpful to implement the power modulation for a certain operating time. This ensures that the DC link voltage stays constant even in the event of Partial Shading Conditions (PSC) for the PV array [26, 27]. Converters are the key component of PV systems, which regulate the power supply by changing its form to enable suitable power transmission and delivery [28]. The controller is specifically made to meet the needs of a buck DC to DC converter structure in terms of simplicity and best performance. To effectively enforce the system to function at the specified reference, the controller is expressly created by developing an appropriate reference model that encapsulates the required characteristics of the Buck converter [29]. The PID controller can control the buck converter's performance [30]. To improve the energy quality, a three-phase voltage source inverter connects the PV system to the grid utility via an LCL filter [31]. By projecting future consumption of items that the utility will transmit or deliver, load estimation lowers

utility risk. The main benefit of forecasting load is that it gives the utility provider information about future load demand and consumption, which helps them to create efficient preparations. Demand forecasting helps create a regulated power grid system and reduces the cost of electricity generation [32, 33]. New hybrid approaches that combine deep learning and machine learning have just been released. The outcomes demonstrate that the hybrid models outperform the traditional models by a considerable margin [34]. The ANN method lowers the mean absolute percentage error in comparison to the Particle Swarm Optimization-based ANN (PSO-ANN), Regression Tree (RT), Support Vector Machine (SVM), and ANN Algorithms [35]. Determine the mean absolute percentage error and the root-mean-squared error to gauge the models' performance. The outcomes demonstrated how well the models using neural networks predicted short-term demands [26, 36]. The complexity of traditional forecasting models, such as the ARIMA model, which takes into account variations in industrial load, renewable energy output, and real-time consumer behavior, makes it impossible to predict consumption patterns. A dual model architecture, comprising Random Forest (RF) models and Bidirectional Long Short-Term Memory (BiLSTM) networks, can be used to get around this restriction. Because it successfully captures the bidirectional relationships in time series data, BiLSTM alone can handle predicting for the short term. BiLSTM and RF predictions can be combined based on their individual error contributions using a reciprocal weighting approach for mid-term forecasting errors [27]. Combining machine learning models like CatBoost or XGBoost, which effectively handle large feature sets, non-linearity, and categorical data, with optimization techniques like the Arithmetic Optimization Algorithm (AOA), Aquila Optimizer (AO), or Phasor Particle Swarm Optimization (PPSO) for tuning the models' hyperparameters can increase the accuracy of short-term load forecasting. When assessed using error metrics like RMSE and MAPE, experimental results demonstrate that both the CatBoost-AOA model and XGBoost-AOA can demonstrate superior outcomes in short-term forecasting [28].

A hybrid three-layer deep learning model that combines the three can handle data and produce results better than each model alone, despite deep learning models like Prophet, Long Short-Term Memory (LSTM), and Backpropagation Neural Network (BPNN) can be used for short-term load forecasting and secure results with acceptable error margins. By breaking down the time series information into trends and periodic components, the Prophet model effectively captures linear and periodic components. LSTM, which excels in handling sequential information with long-term dependencies, is used to analyze the remaining data. By combining the results from Prophet and LSTM, BPNN can produce the final forecast [29]. Combining machine learning frameworks like Support Vector Regression (SVR) for forecasting short-term loads with optimization techniques like Manta Ray Foraging Optimization (MRFO), Slime Mould Algorithm (SMA), Tug

of War Optimization (TWO), or Moth-Flame Optimization (MFO) can increase the models' efficiency. By combining the SVR with the MRFO algorithm, the best level of accuracy can be obtained. SVR is quite sensitive to the kernel, penalty, and epsilon parameters, even if it can effectively simulate the non-linear relations on its own. By keeping SVR from becoming stuck in local minima, MRFO improves accuracy while assisting in striking a balance between model complexity and precision [30]. Current load forecasting models fall into a number of categories, including machine learning (Random Forest, SVR), deep learning (LSTM, GRU), time series approaches (ARIMA, SARIMA), and hybrid approaches that combine several approaches. In capturing intricate and frequent changes in the load data, both machine learning and deep neural networks are adaptable and incredibly accurate. These models also require a lot of data processing and have high computation costs. Despite their demonstrated ease of use and computational efficiency, time series models are unable to account for abrupt changes, nonlinear trends, and exogenous variables such as the weather. Simultaneously, hybrid models that integrate the advantages of various models can offer a well-rounded strategy that ensures greater accuracy for intricate forecasting if designed carefully [37]. The advanced hybrid algorithm performs well even if the load is non-linear [31].

In order to maximize the benefits of several algorithms while reducing their drawbacks, hybrid predictive models employ a range of forecasting techniques, including XGBoost, LSTM, and ARIMA. Hybrid algorithms perform well in estimating electric load when dealing with complex, nonlinear, and seasonal data. As a result, these models can be used to create correction of error systems that are more accurate, function better, and adapt to shifting load patterns [32]. The study shows how hybrid models may adjust to changing load patterns. Hybrid models outperform traditional models in terms of accuracy and precision [38].

3. Load Forecasting Using ARIMA-XGBoost Hybrid

Forecasting electrical consumption is essential in a smart grid. Electric load forecasting for the short term predicts the load from a few seconds to a few weeks in advance. The suggested approach forecasts electric load one day in advance using an ARIMA-XGBoost ensemble hybrid model. A custom-made real-time dataset of rural households in coastal Kerala is used to train the model. The data collection includes time series statistical measurements on electrical power for a period of 30 days. Details of the dataset are given in Table 1. The data collection includes time series statistical methods on electrical power for a period of 30 days. The suggested model uses ARIMA to capture the dataset's seasonality and trends. The autoregressive, integral, and moving average components (p, d, and q) are then used to configure ARIMA. To discover the optimal values of p, d, and q, grid search is utilized. Table 2 shows the range of parameters explored during grid search.

Table 1. Details of the dataset used for training the model

Parameter	Value
Source	Custom-made dataset from rural households in coastal Kerala.
Size	744 * 2
Time Resolution	1 hour
Preprocessing Techniques Used	Date time parsing and indexing, no resampling.

Table 2. Range of parameters explored during grid search

Parameter	Range or Value
Number of estimators	[50,100]
Maximum depth	[2,3]
Learning Rate	[0.05,0.1]
Total combinations tested	8
p, d, q	[0,3]
Objective Function	Akaike Information Criterion

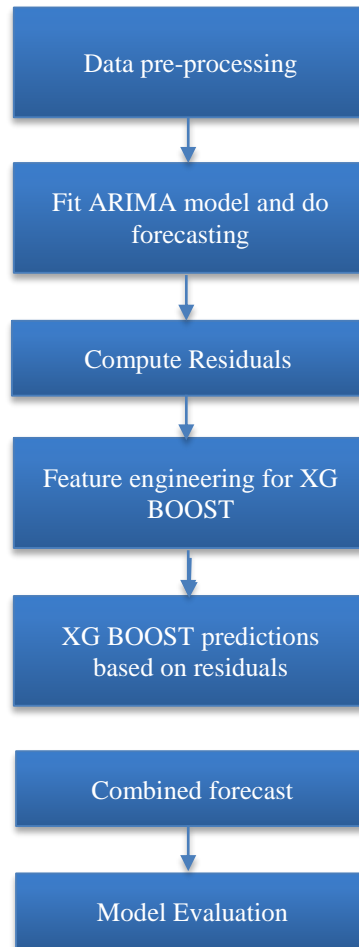
In the proposed work, residuals are found using ARIMA (1), where l_t = observed load at time t , L_{hour} ARIMA's prediction.

$$residual = l_t - larima \quad (1)$$

ARIMA is unable to capture the intricate patterns found in residuals. This is modeled with XGBoost. XGBoost receives rolling mean, delayed residuals, and time-based features as input. Similar to ARIMA grid search, XGBoost hyperparameter optimization is done using grid search. XGBoost reduces residual prediction error. In the suggested model, the forecasting equation is (2), where o = output of the proposed model, yar =ARIMA output, and rxg = residuals predicted by XGBoost.

$$o = yar - rxg \quad (2)$$

This model allows for the distinct modeling of linear and nonlinear patterns, which may be integrated into a single model. Pseudo code for the ARIMA-XGBoost hybrid model is given in Figure 1.

**Fig. 1 Flow chart for ARIMA-XGBoost ensemble hybrid**

4. Nano Grid Design

The nano-grid is an important and vital component of the advancement of smart grids. With scattered energy sources, it is a smaller power system. It is essential to use a system that views the associated generation and loads as a small-scale or subsystem. An interpersonal electrical system with a clear definition of electrical boundaries that operates as a single, controllable unit is called a nano-grid. It is capable of operating in both grid-connected and island modes.

A standalone or isolated nano-grid is a power system that runs entirely off the grid and can be connected to a larger electrical grid. The SIMULINK model of the proposed nano-grid is shown in Figure 2. A boost converter is used to increase the input DC electrical voltage to a preset DC output value. The boost converter specifications and design parameters are listed in Table 3. During Mode 1, Switch is ON, Diode is OFF: IGBT conducts during this period, creating a short circuit between the input's negative supply terminal and the right side of the inductor. Consequently, a current flows through the inductor, which stores energy from its magnetic field, between the negative and positive supply terminals. Since the path directly through the highly conducting IGBT, which has much less impedance than the combination of diode, capacitor, and the load, there is essentially no current flowing in the remaining portion of the circuit. During Mode2, Switch is OFF, Diode is ON: Due to the sudden decrease in current brought on by the IGBT shutting off rapidly, L must produce a back e.m.f. in the opposite direction to the voltage across the inductor during the on period in order to sustain current flow. The voltage from the power source V_d and the back e.m.f. (V_o) Across inductors are thus generated in series.

This elevated voltage forward biases the diode because the MOSFET no longer has a current channel. The load is supplied and the capacitor is charged by the current that emerges from the diode. The voltage across the capacitance in the steady state is equal to the output voltage. The inductor current is continuous, and this is made possible by selecting an appropriate value of inductance. The steady-state inductor current rises from a positive-sloped value to its highest value while in the ON state, then returns to its initial negative-sloped value. Consequently, the inductor current does not change net over the course of a full cycle. Maximum Power Point Tracking, or MPPT, is an algorithm that charge controllers use to extract the maximum amount of power that a photovoltaic module can provide under specific circumstances. In this model, the Perturb and Observe algorithm is used for MPPT. It is also known as the hill-climbing method or the two-point power contrast approach. Only when the PV array's irradiance is constant can it track the power points. The "perturb and observe" technique modifies the voltage while simultaneously keeping an eye on the power output. DC is converted to AC by an inverter. Inverters can use either unipolar or bipolar Sinusoidal Pulse Width Modulation (SPWM). In SPWM, a sine wave (reference) and a triangular wave (carrier) are compared to create pulses. The output is alternated between high (V_s) and low ($-V_s$) voltages in a bipolar switching arrangement for PWM. The switch control for the bipolar scheme is as follows: $S_1 = S_4$ is on when $V_{sine} > V_{tri}$, $S_3 S_2$ is on when $V_{sine} < V_{tri}$. Bipolar PWM's harmonic frequency is $f_h = h \cdot f_1$, where $h = j(mf) \pm k$; $j = 1, 2, 3, \dots$; for each j ; $K = 0, 1, 2, \dots, 24$. Unlike bipolar switching, which switches the output between high and low, unipolar switching for PWM switches the output from a high value to zero or low to zero.

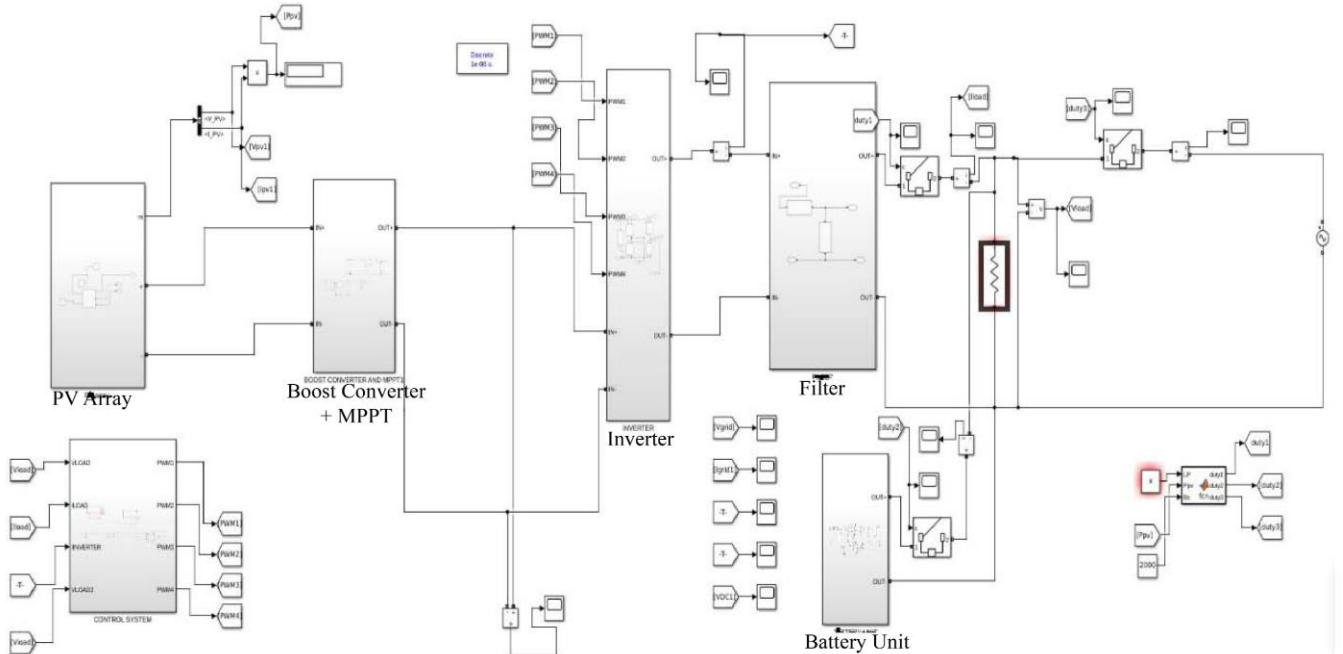


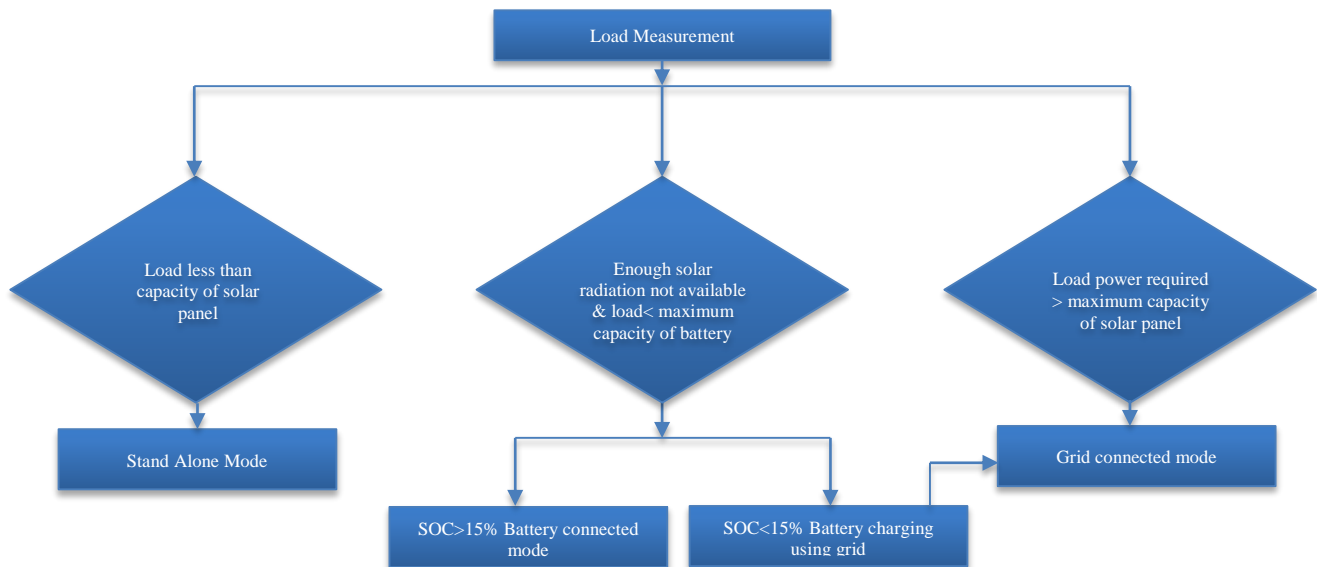
Fig. 2 Simulink model for proposed nano-grid

Table 3. Boost converter design specifications & design parameters

Input voltage (V_{in}) = 230 – 280
Output Voltage (V_{out}) = 400V
Rated Power (P) = 2 kW
Switching frequency (f_{sw}) = 5 kHz
Current ripple (ΔI) = 5%
Voltage ripple (ΔV) = 1%
Input current = $P/V_{in} = 8A$
Current ripple = 5% of Input current = 0.4 A
Voltage ripple = 1% of Output voltage = 4 A
Output Current (I_{out}) = $P/V_{out} = 5A$
Inductance (L) = $(V_{in} * (V_{out} - V_{in})) / (f_{sw} * \Delta I * V_{out}) = 0.0469 H$
Capacitance (C) = $(I_{out} * (V_{out} - V_{in})) / (f_{sw} * \Delta V * V_{out}) = 93.75 \mu F$.

The switch control for the unipolar scheme is as follows. S1 is on when $V_{sine} > V_{tri}$. S1 S3 is on when $V_{sine} < V_{tri}$. S2 is on when $V_{sine} > V_{tri}$. S2 S4 is on when $V_{sine} < V_{tri}$. Harmonic frequency of Unipolar PWM: $f_h = h * f_1$ where $h = j(2mf) \pm k$; $j=1,2,3...$ for each j ; $k=0,1,2,3...$ (if mf is even); $j=1,2,3...$ for each j ; $k=1,2,3...$ (if mf is odd). A bipolar switching scheme is used in this work. Specifications are: Input voltage (V_{in}) = 400 V ; Output voltage (V_{out}) = 220–230 V ; Output power (P_{out}) = 2kW ; Output frequency (f_o) = 50 Hz ; Switching frequency (f_{sw}) = 10 kHz ; Total Harmonic Distortion = < 5% ; Current ripple (ΔI) = 20%. A PI controller is used to process the error between the voltage across the load and the reference sinusoidal waveform, which has a peak value of 230 V. The PI controller's output will provide us with the LC filter's capacitor current. To create the inverter's reference current, combine the capacitor's current with the load current. The voltage that exists across the inductor in the LC filter is then obtained by passing the error created by the reference current and the inverter output current through a PI controller. A reference voltage is created by adding this inductor voltage to the load voltage, and it is

provided to the PWM generator to generate PWM signals. Design of Voltage Control Loop: Control time constant, $T = 200 \mu s$; Capacitor $C = 6.23 \mu F$; Capacitor internal resistance $R_c = 4 \text{ milli ohm}$; Proportionality constant $K_p = C / T = 0.0315$; Integral constant $K_i = R_c / T = 20$. Design of current control loop is as follows: Control time constant, $T = 150 \mu s$; Inductance $L = 4.065 \text{ mH}$; Inductance internal resistance $R_l = 1 \text{ milli ohm}$; Proportionality constant $K_p = L / T = 27.1$; Integral constant $K_i = R_c / T = 6.67 \times 10^{-3}$. Circuits that combine inductors (L) and capacitors (C) to cut or pass particular frequency bands of an electric signal are known as LC filters. At higher frequencies, capacitors facilitate the passage of AC currents while blocking DC currents. On the other hand, at higher frequencies, inductors have a harder time passing AC currents than DC currents. Design of LC filter is as follows: Output current = $P_{out} (\text{Inverter}) / V_{out} (\text{Inverter}) = 2000 / 230 = 8.69 A$; Maximum current ripple = $\Delta I_{ppmax} = 0.2 * \text{Output current} * \text{root}(2) = 2.46 A$ Inductor (L) = $(V_{out} \text{ boost}) / (4 * f_{sw}[\text{inverter}] * \Delta I_{ppmax}) = 4.065 \text{ mH}$; Capacitor (C) = $[(10 * 10) / (2 * \pi * f_{sw}[\text{inverter}])^2] * [1/L] = 6.23 \mu F$.

**Fig. 3 Flow chart of the proposed model**

Five 36 V batteries are connected in series to obtain a voltage of 180 V. The specifications are as follows: Type=Lead-Acid; Nominal voltage=36 V; Rated Capacity=277.5 Ah; Battery response time=0.1 s; Maximum capacity=289.065 Ah; Cut off voltage=27 V; Fully charged voltage=39.1974 V; Nominal discharge current=55.5 A; Internal Resistance=0.0012973 ohm; Capacity at nominal voltage=86.1021 Ah. First, it is necessary to sense the load current, inverter current at the output, and voltage across the load.

A PI controller is then used to transfer the estimated error between the voltage used as the reference and the voltage across the load. The peak of the reference sinusoidal waveform is 230 V. The PI controller will output the current flowing through the capacitor in the LC filter. This capacitor current is combined with the load current to supply the inverter with reference current. An error is then produced between the reference current and the inverter output current in order to obtain the voltage across the inductor in the LC filter. The load and inductor voltages are added to produce a reference voltage. The generator of PWM makes use of this to produce PWM signals.

5. Methodology

To forecast future electric load over a 24-hour period, a bespoke data collection is done initially. The ARIMA-XGBoost hybrid algorithm is trained using this data set. For a 24-hour period, future electric load predictions have been made using the electric load data from the previous 30 days. These predicted loads decide how the Nano-grid should be operated. The standalone Nano-grid's electrical sources are supplemented with an energy storage system.

Integrate a variety of Distributed Generation (DG) sources, especially renewable energy sources. When the connected load in the suggested system is less than 2kW, the maximum power output of the solar panel array at 25 degrees Celsius and 1000 W/m² of radiation—the micro-grid operates in grid-connected mode. In this instance, the circuit breaker between the load and the solar panel stays in the ON position.

A boost converter will increase the DC voltage generated by the solar panel. The boost converter's output is connected to a single-phase inverter, which transforms DC voltage into a square wave voltage. A control system manages the inverter's output power and voltage. To create a sinusoidal voltage with a peak of 220–230 V, the inverter's output is run by means of an LC filter to eliminate harmonics. In this mode, the load receives the power it needs, and the grid receives the remaining power.

If there is insufficient solar radiation at night and the demand is less than the battery's maximum capacity, the battery will be in battery-connected mode. By storing clean

energy generated throughout off-peak hours and supplying it to the electrical grid during times of high demand, batteries give the grid much-needed flexibility. The inverter's output power and voltage are managed by a control system.

In this instance, the circuit breaker between the grid and the battery is in the ON position, as is the circuit breaker between the battery and the load. The battery has a 180 V DC output. An inverter is connected to this DC voltage to transform it into a square wave. An LC filter is applied to the inverter's output to eliminate harmonics and create a sinusoidal voltage waveform.

A transformer is used to step up the 180 V sinusoidal voltage that the LC filter produces to 230 V, which is then sent to the load. Grid-connected micro-grids can function independently in "island mode" when required for practical or technical reasons, but they usually operate synchronously and in conjunction with the traditional wide-area synchronous grid (macro grid). They can supply emergency power and improve the Nano-grid reliability by alternating between linked and island modes.

This kind of system is known as an islandable Nano-grid. When the connected load exceeds the solar panel's maximum capacity of 2 kW at 25 degrees Celsius and radiation equal to 1000 W/m², the solar panel will supply the load with power equal to its maximum capacity; the grid will supply the remaining power. In standalone mode, the MPPT's output is routed to an inverter, while the solar panel's output is routed to the boost converter.

In order to use a voltage controller with 230 volts as a reference, the inverter's output must first produce a square wave, which is subsequently converted to a sine wave by passing through an LC filter. The inverter will receive a PWM from the voltage controller's output. In this case, the load receives enough electricity, and any extra is sent to the grid. In battery-connected mode, the load will only receive power from the battery when the grid and solar panel are turned off. When in grid-connected mode, the photovoltaic array will supply the load with electricity up to its full potential, with the grid supplying the remaining power.

In this case, the load exceeds the solar panel's maximum capacity. At 25 degrees Celsius, the photovoltaic system designed with SIMULINK can produce a maximum of 2097 W of power. There is 1000 W/m² of irradiance. As a result, the solar panel will supply the maximum capacity, with the grid providing the remaining amount. In all cases, the power factor is assumed to be unity.

The Nano-grid will operate in standalone mode if the anticipated load at any given time is less than the solar panel's maximum capacity. The grid and battery will be cut off from the load as a result. If the anticipated load at a given time is

less than the battery's maximum capacity, there is insufficient solar radiation (for example, at night), and the battery's State Of Charge (SOC) is higher than 15%, the Nano grid switches to battery-connected mode.

If the anticipated load at a given time is less than the battery's maximum capacity, there is insufficient solar radiation (for example, at night), and the battery's State Of Charge (SOC) is less than 15%, the battery will be charged using solar panel or grid based on availability of power, as soon as prediction is made by algorithm, so that battery will be having enough charge when it is required to operate. The battery or solar panel will supply power up to its maximum capacity if the anticipated load power at a given time exceeds it; the grid will supply the remaining power. The overall workflow of the model is given in Figure 3.

6. Results

The seasonality and trends of the dataset are captured by the proposed model using ARIMA. ARIMA is then configured using the autoregressive, integral, and moving average components (p, d, and q). Grid search is used to find the ideal values of p, d, and q. Table 4 shows the ideal parameters found using grid search optimization.

Table 4. Ideal parameters found using grid search optimization

Parameter	Best Value
p (ARIMA)	2
d (ARIMA)	1
q (ARIMA)	2
Learning Rate (XGBoost)	0.1
Maximum Depth (XGBoost)	3
Number of Estimators (XGBoost)	100

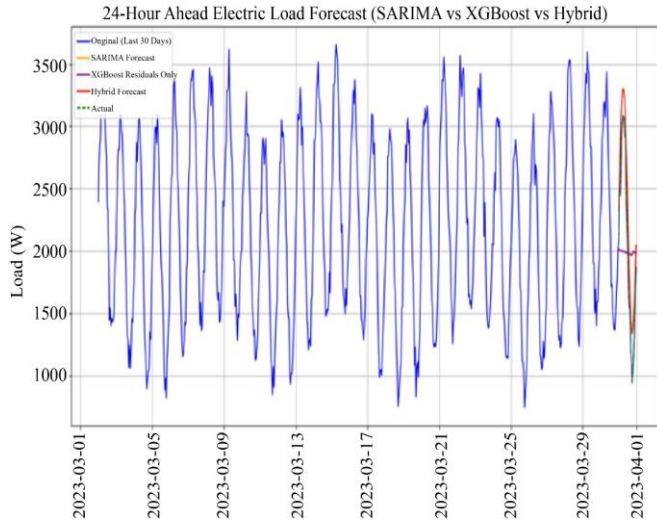


Fig. 4 Load Predictions for 24 hours using the proposed algorithm

ARIMA cannot handle the intricate patterns found in residuals. This is modeled using XGBoost. XGBoost is fed delayed residuals, rolling means, and time - based

characteristics. Similar to ARIMA grid search, grid search is used for XGBoost hyperparameter tuning. Figure 4 shows the estimated power consumption 24 hours ahead of time using the proposed algorithm. The proposed model's comparison with the separate ARIMA and XGBoost techniques is shown in Table 5. The metrics used for comparison are Mean Absolute Error (MAE), Mean Absolute Percentage Error (MAPE), and Root Mean Square Error (RMSE). This predicted data is used to control the operation of the grid under different conditions.

Case 1: The nano-grid will operate in standalone mode if the projected need at any given time is less than the solar panel's maximum capacity. However, only duty 1 (the excitation signal given to the circuit breaker connected between the solar panel and load will have a higher value when the demand is less than the solar panel's maximum capacity. Duty 2 (the excitation signal given to the circuit breaker connected between battery and load) and duty 3 (the excitation signal given to the circuit breaker connected between grid and load) will stay at zero.

Case 2: The nanogrid transitions to battery-connected mode if the expected load at a given moment is less than the battery's highest capacity, there is inadequate solar radiation (for instance, at night), and the battery's State Of Charge (SOC) is greater than 15%. In this case, duty 2 will be high, and duty 1 and duty 3 will be low. For instance, our predictions indicate that the microgrid will operate in the above mode on March 30, 2023, at 10:15 p.m., when the load is 1886W and it is nighttime.

Case 3: The battery will be charged utilizing a solar panel or the grid, based on power availability. As soon as an algorithm predicts that the battery's State Of Charge (SOC) is less than 15%, the predicted load at the given moment is less than the battery's maximum capacity, or there is insufficient solar radiation (e.g., at night). This guarantees that the battery will.

Case 4: If the expected load power at any given time is greater than the battery's or solar panel's maximum capacity, the grid will provide the leftover power at that particular time automatically. Table 6 shows the power flow, where P_{sm} is the Maximum capacity of the solar panel, P_s =Power delivered by the solar panel to the load, P_{g+} =power delivered by the grid to the load, P_b =Power delivered by the battery to the load, and P_{g-} =power delivered to the grid. Solar panel provides power equal to 2097W, and the remaining power, which is 1000W, is delivered by the grid.

Table 5. Optimal Parameters ARIMA and XG BOOST

Model	MAE	RMSE	MAPE
ARIMA	261.69	278.58	15.04%
XGBoost (Residuals only)	627.44	709.03	35.65%
Proposed Model	260.41	277.72	13.67%

Table 6. Power flow of the proposed nano-grid for irradiance 1000W/m²

Load	P _{sm}	P _s	P _{g+}	P _b	P _{g-}
1000W	2097W	1000W	0W	0W	1097W
1500W	2097W	1500W	0W	0W	597W
3000W	2097W	2097W	903W	0W	0W
1000W (SOC < 15%)	0W	0W	0W	1000W	0W

Be sufficiently charged to operate when needed (time at which battery connected mode is predicted). To demonstrate this, we have set the SOC of the battery below 15% before simulation, so that the battery will get charged before night.

7. Conclusion

Simulation software is one of the best tools for the analysis of an integrated nano-grid. This can be used during the conceptual design phase and throughout the nano-grid's lifespan. The simulation and optimization of a complex system is done in an easy manner. The load prediction using

ARIMA-XGBoost ensemble hybrid shows better performance; MAE is 260.41, RMSE is 277.72, and MAPE is 13.67%. The simulation results indicated that the overall system shows a viable solution for load prediction in electric grids. This predicted load is then used to control the operation of the microgrid. The predicted load determines whether the nano-grid must operate in grid-connected mode or stand-alone mode. This control, based on prediction, helps in automation as well as to improve the resilience of the Nano-grid, hence helping the power sector to take one more step towards sustainability.

7.1. Future Scope

In the proposed work, the focus was entirely on controlling the power flow in a nano-grid. Factors such as ethical considerations, data privacy, and cybersecurity are not considered. In the future, researchers can focus on these factors to enable the proposed method to be employed in a real-time scenario.

References

- [1] Saad Ahmad et al., "A Review of Microgrid Energy Management and Control Strategies," *IEEE Access*, vol. 11, pp. 21729-21757, 2023. [\[CrossRef\]](#) [\[Google Scholar\]](#) [\[Publisher Link\]](#)
- [2] M.Y. Arafat, M.J. Hossain, and Md Morshed Alam, "Machine Learning Scopes on Microgrid Predictive Maintenance: Potential Frameworks, Challenges, and Prospects," *Renewable and Sustainable Energy Reviews*, vol. 190, 2024. [\[CrossRef\]](#) [\[Google Scholar\]](#) [\[Publisher Link\]](#)
- [3] Monika Sandelic et al., "Reliability Aspects in Microgrid Design and Planning: Status and Power Electronics-Induced Challenges," *Renewable and Sustainable Energy Reviews*, vol. 159, pp. 1-17, 2022. [\[CrossRef\]](#) [\[Google Scholar\]](#) [\[Publisher Link\]](#)
- [4] Erik Ela et al., "Evolution of Operating Reserve Determination in Wind Power Integration Studies," *IEEE PES General Meeting*, Minneapolis, MN, USA, pp. 1-8, 2010. [\[CrossRef\]](#) [\[Google Scholar\]](#) [\[Publisher Link\]](#)
- [5] Jana Gerlach, Sarah Eckhoff, and Michael H. Breitner, "Decision Support for Strategic Microgrid Design Integrating Governance, Business, Intelligence, Communication, and Physical Perspectives," *Sustainable Cities and Society*, vol. 113, pp. 1-19, 2024. [\[CrossRef\]](#) [\[Google Scholar\]](#) [\[Publisher Link\]](#)
- [6] Abed Kazemtarghi, and Ayan Mallik, "Techno-Economic Microgrid Design Optimization Considering Fuel Procurement Cost and Battery Energy Storage System Lifetime Analysis," *Electric Power Systems Research*, vol. 235, pp. 1-31, 2024. [\[CrossRef\]](#) [\[Google Scholar\]](#) [\[Publisher Link\]](#)
- [7] Rolando J. Tremont-Brito, Rachid Darbali-Zamora, and Erick E. Aponte-Bezarez, "Implementing Extreme Events, Hazards and Fragility Data, and Mitigation Trade-Off Analysis Using the Microgrid Design Toolkit for a Rural Community in Puerto Rico," *2024 IEEE 52nd Photovoltaic Specialist Conference (PVSC)*, Seattle, WA, USA, pp. 0926-0932, 2024. [\[CrossRef\]](#) [\[Google Scholar\]](#) [\[Publisher Link\]](#)
- [8] Mark Vygoder et al., "A Novel Protection Design Process to Increase Microgrid Resilience," *IEEE Transactions on Industry Applications*, vol. 60, no. 4, pp. 5372-5387, 2024. [\[CrossRef\]](#) [\[Google Scholar\]](#) [\[Publisher Link\]](#)
- [9] Sheeba T. Blesslin et al., *Microgrid Optimization and Integration of Renewable Energy Resources: Innovation, Challenges and Prospects*, Integration of Renewable Energy Sources with Smart Grid, Wiley, pp. 239-262, 2021. [\[CrossRef\]](#) [\[Google Scholar\]](#) [\[Publisher Link\]](#)
- [10] C. Siddaraju, S. Deepak, and H.S. Balasubramanya, "Optimal Design of Smart Grid Renewable Energy System using Homer Programme," *Journal of Mines, Metals and Fuels*, vol. 70, no. 3A, pp. 134-137, 2022. [\[CrossRef\]](#) [\[Google Scholar\]](#) [\[Publisher Link\]](#)
- [11] M.A. Ebrahim et al., "Electric Eel Foraging Optimization-Based Control Design of Islanded Microgrid," *Scientific Reports*, vol. 15, no. 1, pp. 1-22, 2025. [\[CrossRef\]](#) [\[Google Scholar\]](#) [\[Publisher Link\]](#)
- [12] Joy Dalmacio Billanes, Bo Nørregaard Jørgensen, and Zheng Ma, "A Framework for Resilient Community Microgrids: Review of Operational Strategies and Performance Metrics," *Energies*, vol. 18, no. 2, pp. 1-39, 2025. [\[CrossRef\]](#) [\[Google Scholar\]](#) [\[Publisher Link\]](#)
- [13] Shama Naz Islam, and Md Apel Mahmud, "Communication Protocol Design for IoT-Enabled Energy Management in a Smart Microgrid," *Applied Sciences*, vol. 15, no. 4, pp. 1-22, 2025. [\[CrossRef\]](#) [\[Google Scholar\]](#) [\[Publisher Link\]](#)
- [14] Afam Uzorka et al., "Design and Implementation of a Photovoltaic System for Health Facilities in Rural Areas of Uganda," *Discover Applied Sciences*, vol. 7, no. 3, pp. 1-12, 2025. [\[CrossRef\]](#) [\[Google Scholar\]](#) [\[Publisher Link\]](#)

- [15] Omkar Singh, Anjan Kumar Ray, and Arabinda Ghosh, "Photovoltaic Module Performance: Modeling, Parameter Estimation, and Environmental Effects," *e-Prime-Advances in Electrical Engineering, Electronics and Energy*, vol. 8, pp. 1-14, 2024. [[CrossRef](#)] [[Google Scholar](#)] [[Publisher Link](#)]
- [16] Mohammad Reza Maghami, Jagadeesh Pasupuleti, and Janaka Ekanayake, "Energy Storage and Demand Response as Hybrid Mitigation Technique for Photovoltaic Grid Connection: Challenges and Future Trends," *Journal of Energy Storage*, vol. 88, 2024. [[CrossRef](#)] [[Google Scholar](#)] [[Publisher Link](#)]
- [17] Runze Lv, Yinxiao Zhu, and Yongheng Yang, "Robust Design of Perturb & Observe Maximum Power Point Tracking for Photovoltaic Systems," *IEEE Transactions on Industry Applications*, vol. 60, no. 4, pp. 6547-6558, 2024. [[CrossRef](#)] [[Google Scholar](#)] [[Publisher Link](#)]
- [18] M. Manohara et al., "Analysis of Perturb & Observe MPPT Algorithm in Partial Shading for DC-DC Boost Converters," *2024 Second International Conference on Smart Technologies for Power and Renewable Energy (SPECon)*, Ernakulam, India, pp. 1-4, 2024. [[CrossRef](#)] [[Google Scholar](#)] [[Publisher Link](#)]
- [19] Fevzi Çakmak, Zafer Aydoğmuş, and Mehmet Rıda Tür, "Analysis of Open Circuit Voltage MPPT Method with Analytical Analysis with Perturb and Observe (P&O) MPPT Method in PV Systems," *Electric Power Components and Systems*, vol. 52, no. 9, pp. 1528-1542, 2023. [[CrossRef](#)] [[Google Scholar](#)] [[Publisher Link](#)]
- [20] G. Gabriel Santhosh Kumar, and S. Titus, "Hybrid Artificial Rabbit Optimization and Perturb & Observe MPPT for Grid-Connected PV System," *Electric Power Components and Systems*, vol. 52, no. 11, pp. 2008-2029, 2023. [[CrossRef](#)] [[Google Scholar](#)] [[Publisher Link](#)]
- [21] H.S. Sridhar, and Kc Sakshith Devaiah, "Modelling and Analysis of Voltage Mode Control (VMC) of Buck Converter using P, PI, PID Controller," *2024 International Conference on Smart Systems for Applications in Electrical Sciences (ICSSES)*, Tumakuru, India, pp. 1-5, 2024. [[CrossRef](#)] [[Google Scholar](#)] [[Publisher Link](#)]
- [22] Wenqiang Zhu, "A Novel Simplified Buck Power System Control Algorithm: Application to the Emulation of Photovoltaic Solar Panels," *Computers and Electrical Engineering*, vol. 116, 2024. [[CrossRef](#)] [[Google Scholar](#)] [[Publisher Link](#)]
- [23] Ahmad Saudi Samosir, Tole Sutikno, and Luthfiyyatun Mardiyah, "Simple Formula for Designing the PID Controller of a DC-DC Buck Converter," *International Journal of Power Electronics and Drive Systems*, vol. 14, no. 1, pp. 327-336, 2023. [[CrossRef](#)] [[Google Scholar](#)] [[Publisher Link](#)]
- [24] J. Suganya, R. Karthikeyan, and J. Ramprabhakar, *Voltage Stabilization by Using Buck Converters in the Integration of Renewable Energy into the Grid*, New Trends in Computational Vision and Bio-inspired Computing, Springer, Cham, pp. 509-517, 2020. [[CrossRef](#)] [[Google Scholar](#)] [[Publisher Link](#)]
- [25] Ghriissi Tahri, Fatima Tahri, and Ali Tahri, "PID Control Based on PSO for a Grid Connected Photovoltaic System using a Three-Phase Voltage Source Inverter," *2024 3rd International Conference on Advanced Electrical Engineering (ICAEE)*, Sidi-Bel-Abbes, Algeria, pp. 1-6, 2024. [[CrossRef](#)] [[Google Scholar](#)] [[Publisher Link](#)]
- [26] Waqar Waheed, and Qingshan Xu, "Data-Driven Short Term Load Forecasting with Deep Neural Networks: Unlocking Insights for Sustainable Energy Management," *Electric Power Systems Research*, vol. 232, 2024. [[CrossRef](#)] [[Google Scholar](#)] [[Publisher Link](#)]
- [27] Feifei Yang et al., "Decomposition Strategy and Attention-Based Long Short-Term Memory Network for Multi-Step Ultra-Short-Term Agricultural Power Load Forecasting," *Expert Systems with Applications*, vol. 238, 2024. [[CrossRef](#)] [[Google Scholar](#)] [[Publisher Link](#)]
- [28] Hongsheng Xu et al., "Construction and Application of Short-Term and Mid-Term Power System Load Forecasting Model Based on Hybrid Deep Learning," *IEEE Access*, vol. 11, pp. 37494-37507, 2023. [[CrossRef](#)] [[Google Scholar](#)] [[Publisher Link](#)]
- [29] Lijie Zhang, and Dominik Jánošík, "Enhanced Short-Term Load Forecasting with Hybrid Machine Learning Models: Cat Boost and XGBoost Approaches," *Expert Systems with Applications*, vol. 241, 2024. [[CrossRef](#)] [[Google Scholar](#)] [[Publisher Link](#)]
- [30] Tasarruf Bashir et al., "Short Term Electricity Load Forecasting using Hybrid Prophet-LSTM Model Optimized by BPNN," *Energy Reports*, vol. 8, pp. 1678-1686, 2022. [[CrossRef](#)] [[Google Scholar](#)] [[Publisher Link](#)]
- [31] Saima Akhtar et al., "Short-Term Load Forecasting Models: A Review of Challenges, Progress, and the Road Ahead," *Energies*, vol. 16, no. 10, pp. 1-29, 2023. [[CrossRef](#)] [[Google Scholar](#)] [[Publisher Link](#)]
- [32] M. Mithun Krishnan, and K.R. Bharath, "A Novel Sensorless Hybrid MPPT Method Based on FOCV Measurement and P&O MPPT Technique for Solar PV Applications," *2019 International Conference on Advances in Computing and Communication Engineering (ICACCE)*, Sathyamangalam, India, pp. 1-5, 2019. [[CrossRef](#)] [[Google Scholar](#)] [[Publisher Link](#)]
- [33] G. Jayachitra et al., "Fuzzy Based Perturb & Observe MPPT Algorithm for Grid Tied PV System," *2023 IEEE International Conference on Distributed Computing, VLSI, Electrical Circuits and Robotics (DISCOVER)*, Mangalore, India, pp. 123-127, 2023. [[CrossRef](#)] [[Google Scholar](#)] [[Publisher Link](#)]
- [34] A. Peer Mohamed et al., "Adaptive Maximum Power Extraction Technique in Fuel-Cell Integrated with Novel DC-DC Converter Topology for Low-Power Electric Vehicle Applications," *Engineering Science and Technology, an International Journal*, vol. 54, pp. 1-20, 2024. [[CrossRef](#)] [[Google Scholar](#)] [[Publisher Link](#)]
- [35] Juyong Lee, and Youngsang Cho, "National-Scale Electricity Peak Load Forecasting: Traditional, Machine Learning, or Hybrid Model?," *Energy*, vol. 239, pp. 1-42, 2022. [[CrossRef](#)] [[Google Scholar](#)] [[Publisher Link](#)]

- [36] Gomathinayagam Indira et al., “Electricity Load Demand Prediction for Microgrid Energy Management System using Hybrid Adaptive Barnacle-Mating Optimizer with Artificial Neural Network Algorithm,” *Energy Technology*, vol. 12, no. 5, 2024. [[CrossRef](#)] [[Google Scholar](#)] [[Publisher Link](#)]
- [37] Siwei Li et al., “Short-Term Electrical Load Forecasting using Hybrid Model of Manta Ray Foraging Optimization and Support Vector Regression,” *Journal of Cleaner Production*, vol. 388, 2023. [[CrossRef](#)] [[Google Scholar](#)] [[Publisher Link](#)]
- [38] Yusha Hu et al., “Industrial Artificial Intelligence-Based Energy Management System: Integrated Framework for Electricity Load Forecasting and Fault Prediction,” *Energy*, vol. 244, pp. 1-46, 2022. [[CrossRef](#)] [[Google Scholar](#)] [[Publisher Link](#)]
- [39] C. Jeevakarunya, and V. Manikandan, “Advanced Machine Learning Approach with Dynamic Kernel Weighting for Accurate Electrical Load Forecasting,” *AIP Advances*, vol. 15, no. 1, pp. 1-14, 2025. [[CrossRef](#)] [[Google Scholar](#)] [[Publisher Link](#)]